Profiling sterols in cerebrotendinous xanthomatosis: Utility of Girard derivatization and high resolution exact mass LC–ESI-MS^n analysis☆

Andrea E. DeBarber [a,*], Yana Sandlers [b], Anuradha S. Pappu [a,c], Louise S. Merkens [c], P. Barton Duell [d], Steven R. Lear [e], Sandra K. Erickson [e,f], Robert D. Steiner [g]

[a] Department of Physiology and Pharmacology, Oregon Health & Science University (OHSU), Portland, OR 97239, United States
[b] Biochemical Genetics Laboratory, Kennedy Krieger Institute, Baltimore, MD 21205, United States
[c] Department of Pediatrics, OHSU, United States
[d] Department of Medicine, Division of Endocrinology, Diabetes and Clinical Nutrition, OHSU, United States
[e] Department of Veterans Affairs Medical Center (VAMC), San Francisco, CA 94121, United States
[f] Department of Medicine/Endocrinology and Metabolism, University of California, San Francisco, CA 94121, United States
[g] Departments of Pediatrics and Molecular & Medical Genetics, Child Development and Rehabilitation Center, Doernbecher Children's Hospital, OHSU, United States

ARTICLE INFO

ABSTRACT

In this study we profile free 3-oxo sterols present in plasma from patients affected with the neurodegenerative disorder of sterol and bile acid metabolism cerebrotendinous xanthomatosis (CTX), utilizing a combination of charge-tagging and LC–ESI-MS^n performed with an LTQ-Orbitrap Discovery instrument. In addition, we profile sterols in plasma from 24-month-old cyp27A1 gene knockout mice lacking the enzyme defective in CTX. Charge-tagging was accomplished by reaction with cationic Girard's P (GP) reagent 1-(carboxymethyl) pyridinium chloride hydrazide, an approach uniquely suited to studying the 3-oxo sterols that accumulate in CTX, as Girard's reagent reacts with the sterol oxo moiety to form charged hydrazone derivatives. The ability to selectively generate GP-tagged 3-oxo-4-ene and 3-oxo-5(H) saturated plasma sterols enabled ESI-MS^n analysis of these sterols in the presence of a large excess (3 orders of magnitude) of cholesterol. Often cholesterol detected in biological samples makes it challenging to quantify minor sterols, with cholesterol frequently removed prior to analysis. We derivatized plasma (10 μl) without SPE removal of cholesterol to ensure detection of all sterols present in plasma. We were able to measure 4-cholesten-3-one in plasma from untreated CTX patients (1207 ± 302 ng/ml, mean $\pm$ SD, $n = 4$), as well as other intermediates in a proposed pathway to 5α-cholestanol. In addition, a number of bile acid precursors were identified in plasma using this technique. GP-tagged sterols were identified utilizing high resolution exact mass spectra (± 5 ppm), as well as MS^2 ([M]$^+ \rightarrow$) spectra that possessed characteristic neutral loss of 79 Da (pyridine) fragment ions, and MS^3 ([M]$^+ \rightarrow$ [M−79]$^+ \rightarrow$) spectra that provided additional structurally informative fragment ions.

© 2010 Elsevier B.V. All rights reserved.

1. Introduction

Cerebrotendinous xanthomatosis (CTX; OMIM#213700) is a rare genetic disorder associated with deficient sterol 27-hydroxylase (CYP27A1); an enzyme important in the conversion of cholesterol to cholic and chenodeoxycholic acid (CDCA) (Fig. 1 neutral pathway to primary bile acids). A damaging consequence of CYP27A1 deficiency is the accumulation of 5α-cholestanol (a 5α-dihydro derivative of cholesterol) in the tissues of affected patients. Patients often develop 5α-cholestanol and cholesterol containing xanthomas. Extensive deposition of 5α-cholestanol in the brain [1],

is associated with the development of severe neurological dysfunction. In addition to 5α-cholestanol, tissues and blood from untreated CTX patients contain high concentrations of bile acid precursors, in particular 7α-hydroxy-4-cholesten-3-one (C4-7α-ol-3-one, see Fig. 1) [2–8].

The data reported thus far suggest that a major synthetic pathway to 5α-cholestanol in CTX patients originates from C4-7α-ol-3-one [9], in contrast to a normal synthetic pathway that originates from cholesterol. Both pathways for 5α-cholestanol synthesis appear to converge through 4-cholesten-3-one (C4-3-one, Fig. 1). *In vivo* studies in CTX patients demonstrated the formation of biliary 5α-cholestanol from intravenous dosed [^{14}C]-labeled C4-3-one [10]. Studies in rabbits [11] and in rats [12] demonstrated that 5α-cholestanol was rapidly found in circulation after oral dosing with [^{14}C]-labeled C4-3-one. Interestingly, prolonged feeding of C4-3-one (0.5%) in birds resulted in severe aortic arteriosclerosis and the accumulation of large amounts of 5α-cholestanol in blood
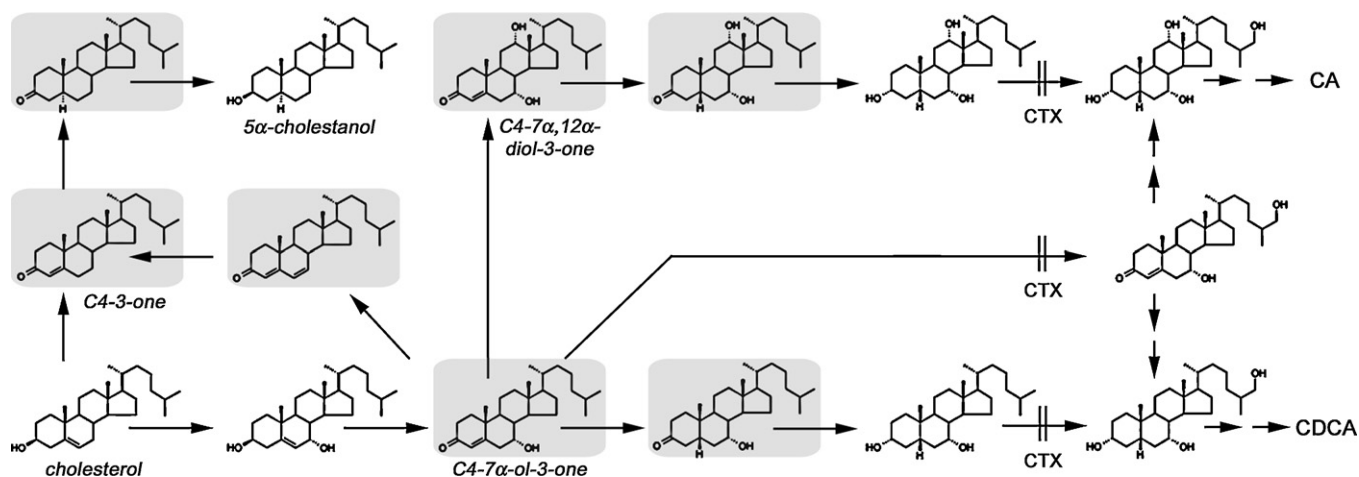
Fig. 1. The neutral pathway to primary bile acids in cerebrotendinous xanthomatosis (CTX). Bile acid precursors (bile alcohols) are generated by increased cholesterol 7α-hydroxylase activity, in addition to deficient 27-hydroxylation in CTX affected patients. With CDCA treatment of CTX the plasma concentration of 7α-hydroxy-4-cholesten-3-one (C4-7α-ol-3-one) rapidly declines [8,9]; reflecting feedback inhibition by CDCA to decrease cholesterol 7α-hydroxylation, and limit bile acid synthesis [9]. In the normal sequence of events C4-7α-ol-3-one can be further hydroxylated to form 7α,12α-dihydroxy-4-cholesten-3-one (C4-7α,12α-diol-3-one). Both C4-7α,12α-diol-3-one and C4-7α-ol-3-one are reduced by a soluble 3-oxosteroid Δ4-steroid 5β-reductase to form 7α,12α-dihydroxy-5β-cholestan-3-one and 7α-hydroxy-5β-cholestan-3-one, respectively [9]. Prior to 27-hydroxylation the 3-oxo moiety in each bile alcohol is further reduced by a 3α-hydroxysteroid dehydrogenase to form 5β-cholestane-3α,7α,12α-triol and 5β-cholestane-3α,7α-diol respectively [9].

and tissues [12,13]. The synthesis of 5α-cholestanol from C4-3-one was demonstrated to occur *via* 5α-cholestan-3-one under *in vitro* conditions utilizing animal liver tissue preparations [14,15].

Although *in vitro* experiments initially suggested C4-3-one was formed from cholesterol in CTX [10], more recent studies indicate a major pathway to C4-3-one in CTX is formation from 4,6-cholestadiene-3-one produced from C4-7α-ol-3-one (Fig. 1) [2,7]. High concentrations of 4,6-cholestadiene-3-one (500–850 ng/ml) were shown to be present in hydrolyzed serum from untreated CTX patients [2], and the turnover of 4,6-cholestadiene-3-one to C4-3-one and 5α-cholestanol was demonstrated in liver and brain tissue studies [16]. Although C4-7α-ol-3-one can undergo non-enzyme catalyzed dehydration to form 4,6-cholestadiene-3-one, *in vitro* studies with liver tissue have characterized enzymatic conversion of C4-7α-ol-3-one to 4,6-cholestadiene-3-one and subsequent saturation of the Δ-6 double bond to form C4-3-one [3,17].

To provide insight into alternate pathways that may be accentuated when bile acid synthesis is perturbed in CTX, we hypothesized a recently described approach utilizing the hybrid Thermo LTQ-Orbitrap instrument coupled with sterol derivatization [18] could be utilized for highly sensitive, selective ESI-MS^n analysis of 3-oxo-4-ene sterols present in blood and tissues of CTX patients. The approach involves sterol derivatization with cationic Girard's P (GP) reagent to enhance ESI ionization, as well as to provide MS^2 ([M]$^+$→) spectra fragment ions possessing characteristic GP derivative neutral losses of 79 and 107 Da [18,19] and MS^3 ([M]$^+$ → [M−79]$^+$→) spectra fragment ions that provide further structural information. The Girard derivatives are resolved using HPLC and are identified by exact mass analysis (±5 ppm), with MS^2 and MS^3 spectra obtained to confirm sterol identity. Exact mass data is generated in the Orbitrap mass analyzer and MS^n spectra are generated in the LTQ linear ion trap (LIT) mass analyzer. We set out to detect sterols possessing a 3-oxo-4-ene or 3-oxo-5(H) saturated structure proposed to be *in vivo* intermediates in CTX biochemical pathways (Fig. 1) in a targeted manner utilizing derivatization with GP reagent and LC–ESI-MS^n analysis with an LTQ-Orbitrap Discovery instrument. We undertook this effort as part of a larger project designed to investigate altered metabolic pathways in CTX, in order to develop improved methods of screening, diagnosis, and treatment for this disorder. We describe here profiling of the free 3-oxo sterols present in plasma from affected patients and from 24-month-old cyp27A1 gene knock out (cyp27A1 −/−) mice deficient in sterol 27-hydroxylase, the enzyme defective in CTX [5,20,21]. Bile acid precursors are elevated in these mice, which display a 3- to 5-fold increase in cholesterol 7α-hydroxylase activity [22]. Although large amounts of C4-7α-ol-3-one are present in liver tissue and blood from the mice [5,20], they do not develop xanthomas, or accumulate 5α-cholestanol to the extent observed in human disease [5,22,23]. Recently, significant cerebral accumulation of 5α-cholestanol was noted to occur in 12-month-old cyp27A1 −/− mice, especially in female mice [20], although corresponding to only 3% of the sterol pool versus 20–40% in patients with CTX [24]. The cyp27A1 −/− mice were used to demonstrate formation of cerebral 5α-cholestanol from intravenously dosed [^{2}H]-labeled C4-7α-ol-3-one [20].

To summarize, in this study we report on the utility of GP derivatization and high resolution exact mass LC–ESI-MS^n analysis for profiling the free 3-oxo sterols present in plasma from untreated CTX patients and cyp27A1 −/− mice. We previously examined the utility of GP derivatization for quantitative LC–ESI-MS^2 analysis of a specific 3-oxo-4-ene sterol elevated in plasma from CTX patients [2–8]; C4-7α-ol-3-one. We found C4-7α-ol-3-one demonstrated improved utility as a diagnostic marker of disease and to monitor treatment compared to 5α-cholestanol [8]. We anticipate GP-tagged sterols identified with high resolution exact mass LC–ESI-MS^n analysis will be amenable to LC–ESI-MS^2 analysis performed with unit resolution instrumentation as previously described for C4-7α-ol-3-one [8], and we describe here preliminary LC–ESI-MS^2 experiments to measure 5α-cholestanol precursors We discuss our results in relation to the alternate pathways utilized when bile acid synthesis is perturbed in CTX and in the cyp27A1 −/− mouse.

2. Experimental

2.1. Chemicals and reagents

4,6-Cholestadiene-3-one, 5α-cholestan-3β-ol (5α-cholestanol), 5α-cholestan-3-one, 4-cholesten-3-one (C4-3-one), cholesterol (5-cholesten-3β-ol), 7α-hydroxy-4-cholesten-3-one (C4-7α-ol-3-one) and 3α,7α,12α-trihydroxy-5β-cholestane were from Steraloids (Newport, RI). 5β-Cholestan-3α-ol (5β-

cholestanol) was obtained from Sigma–Aldrich (St Louis, MO). 7α,12α-Dihydroxy-5β-cholestan-3-one was synthesized from 3α,7α,12α-trihydroxy-5β-cholestane using 3α-hydroxysteroid dehydrogenase from Sigma–Aldrich in the presence of β-NAD [25]. C4-7α-ol-3-one-d_7 and C4-3-one-d_7 internal standards were synthesized from their respective 3β-hydroxy-Δ5 analogues using *Stretomyces* sp. cholesterol oxidase obtained from Sigma–Aldrich as described previously [8,26,27]. 7α-Hydroxycholesterol-d_7 and cholesterol-d_7 were obtained from CDN Isotopes (Pointe-Claire, Quebec, Canada). Methanol and water (GC–MS grade) were from Burdick and Jackson (Muskegon, MI). Formic acid (90%) was J.T. Baker brand and glacial acetic acid (99.99%) was from Aldrich. 'Girard's reagent P' (1-(carboxymethyl)pyridinium chloride hydrazide) was obtained from TCI America (Portland, OR). Volume 0.5 ml Ultrafree-MC centrifugal filters (0.45 μm) were from Millipore (Bedford, MA). Human pooled plasma (K$_2$EDTA) was purchased from Biological Specialty Corporation (Colmar, PA).

2.2. Human and animal studies

Informed consent was obtained from the CTX patients and patient study protocols were approved by the Oregon Health & Science University Institutional Review Board. Blood samples were collected from untreated patients aged >16 years (n = 4). Blood was collected from both male and female cyp27A1 gene knock out mice and their wild type littermates at 24 months of age. Plasma (K$_2$EDTA) was separated from the blood samples and stored at $-80\,^\circ$C. The cyp27A1 $-/-$ and cyp27A1 wild type (+/+) mice were from a heterozygote breeding colony at the Department of Veterans Affairs Medical Center San Francisco (VAMC), which was transferred onto the C57BL/6J background by backcrossing more than 10 generations [22]. Mouse study protocols were approved by the Animal Studies Subcommittee, VAMC San Francisco. The animals were maintained on rodent chow and fed ad libitum. The Animal Research Facility at VAMC San Francisco is specific pathogen free and is 'Association for Assessment and Accreditation of Laboratory Animal Care International' accredited.

2.3. Preparation of calibrators and samples

Calibrators for the GC–FID and GC–MS methods were generated using dilutions of cholesterol and 5α-cholestanol authentic standard in *n*-propyl alcohol or chloroform. To measure cholesterol and 5α-cholestanol, plasma samples (25–100 μl) were spiked with internal standard (5β-cholestanol), hydrolyzed, extracted and derivatized to form trimethylsilyl ethers. GC was performed using a Phenomenex ZB1701 column (30 m, ID = 0.25 mm, 0.25 μm) with the method temperature held at 170$\,^\circ$C for 2 min, the temperature increased at 18$\,^\circ$C/min to 260$\,^\circ$C, the temperature held for 12 min and increased at 3C$^\circ$/min to 280$\,^\circ$C. Cholesterol was analyzed by FID and cholestanol by SIM MS; with detection of an m/z = 355.4 target ion for internal standard and m/z = 306.3 ion for 5α-cholestanol. Calibrators for the LC–ESI-MS^n methods were generated using dilutions of C4-7α-ol-3-one, C4-3-one and 5α-cholestan-3-one authentic standard in methanol or by spiking commercially available plasma with authentic standard solution. After addition of 20 μl of methanol containing C4-7α-ol-3-one-d_7 (10 ng) and C4-3-one-d_7 (10 ng) internal standards, sterols present in calibrators or 10 μl plasma samples were derivatized with 175 μl of 10 mM GP reagent in methanol at 1% acetic acid. The samples were shaken (200 rpm) for 120 min at room temperature and for plasma samples the precipitate was removed using centrifugal filters (0.45 μm) prior to LC–ESI-MS^n analysis.

2.4. LC–ESI-MS^n

GP-tagged sterols were resolved using an Accela UPLC system (Thermo Scientific, San Jose, CA) with sample injection volume of 10 μl. Samples were injected onto a Michrom BioResources (Auburn, CA) trap C$_{18}$ cartridge that was subsequently washed at 0.2 ml/min to remove excess GP reagent with solvent consisting of 33% methanol, 17% acetonitrile and 50% water. After 2 min the GP-tagged sterols were back-flushed onto a 50 mm × 2.1 mm, 1.9 μm, Hypersil Gold C$_{18}$-HPLC column from Thermo Hypersil (Waltham, MA, USA). The gradient mobile phase for HPLC separation (modified from Ogundare et al. [28]) was delivered at 0.2 ml/min and consisted of two solvents (both containing 0.1% formic acid); **A** consisting of 33% methanol, 17% acetonitrile and 50% water and **B** consisting of 63% methanol, 32% acetonitrile, 5% water. Solvent **B** was increased from 25% to 100% over 3 min. The column was kept at 100% **B** for 6 min prior to increasing the flow to 0.25 ml/min for 2 min. The column was then equilibrated at 0% **B** for 2 min at 0.25 ml/min, giving a total run time of 15 min. The HPLC eluent was directed to a LTQ-Orbitrap XL Discovery instrument (San Jose, CA, USA), equipped with an ESI ion max source. The ionization interface was operated in the positive mode using the following settings: source voltage, 4 kV; sheath and aux gas flow rates, 50 and 5 units, respectively; tube lens voltage, 90 V; capillary voltage, 49 V; and capillary temperature, 300$\,^\circ$C. The Orbitrap mass analyzer was externally calibrated prior to analysis to obtain mass accuracy within $\pm$5 ppm. An LC–ESI-MS^n method was created to perform three scan events in a data dependent manner as described by Griffiths et al. [18]; a high resolution (30,000) full scan event over the m/z range 600–800 utilizing the Orbitrap analyzer, followed by data-dependent MS^2 and MS^3 events performed in the LIT. For the MS^2 and MS^3 events the normalized collision energies were 30% and 35%, respectively. A precursor ion inclusion list was generated based on the m/z of [M]$^+$ ions for GP derivatives of potential sterols present, and MS^2 spectra were collected if precursor ions were present in the full scan spectra above a threshold of 500 counts. If a [M$-$79]$^+$ fragment ion was observed in MS^2 spectra above a threshold of 200 counts, MS^3 spectra were collected for the [M$-$79]$^+$ ion.

Plasma GP-tagged C4-7α-ol-3-one, C4-3-one and 5α-cholestan-3-one were quantified using calibrators and high resolution data generated with the Orbitrap analyzer or LC–ESI-MS^2 data generated with an Applied Biosystems/SCIEX 4000 QTRAP instrument (Foster City, CA) scanning in triple quadrupole mode. The TurboIonSpray® ESI interface was operated in the positive mode with settings similar to those previously described for detection of GP-tagged C4-7α-ol-3-one [8]. The MRM transitions monitored for GP-tagged C4-7α-ol-3-one, C4-3-one and 5α-cholestan-3-one were m/z 534.4 → 455.4, m/z 518.4 → 439.4 and m/z 520.4 → 441.4, respectively. Collision energies were 40 V, dwell times were 75 ms, and Q1 and Q3 were operated at unit resolution. The UPLC–ESI-MS^2 system was composed of an in-line Shimadzu (Columbia, MD) SIL-20AC XR auto-sampler and 2 LC-20AD XR LC pumps. GP-tagged sterols were resolved with a gradient mobile phase (consisting of water and methanol at 0.1% formic acid) as previously described [8], using a 30 mm × 2.1 mm, 1.9 μm Hypersil Gold C$_{18}$-HPLC column with a 10 mm × 2.1 mm, 3 μm Betabasic C$_{18}$-guard from Thermo Hypersil. LC–APCI-MS^2 analysis of underivatized C4-7α-ol-3-one was performed with the 4000 QTRAP instrument to assess the signal enhancement factor for GP derivatization. The ionization interface was operated in the positive mode using the following settings: source temp (TEM), 450$\,^\circ$C, ion spray needle voltage (IS), 5.0 kV; curtain (CUR), heater (GS1) and nebulizer (GS2) nitrogen gas flow rates, 15, 55 and 20 psi, respectively; declustering potential (DP), 91 V; entrance potential (EP), 10 V; and collision cell exit potential (CXP), 24 V. The MRM transition monitored for was

m/z 401.3→383.3. The collision energy (CE) was 25 V, dwell time was 100 ms and Q1 and Q3 were operated at unit resolution. The LC–APCI-MS^2 system was equipped with a 100×2.1 (ID) mm, 5 μm Betabasic C$_{18}$-HPLC column with a 10 mm × 2.1 mm, 5 μm Betabasic C$_{18}$-guard from ThermoHypersil. The gradient mobile phase was delivered at a flow rate of 0.4 ml/min. The mobile phase consisted of two solvents: **A**, water and 0.1% formic acid, and **B**, methanol, 5 mM ammonium acetate and 0.1% formic acid. Solvent **B** was increased from 60% to 98% over 2 min, the column was washed at 98% **B** for 3 min and re-equilibrated at 60% **B** for 3 min. The LC column temperature was kept at 40 °C using a Shimadzu CTO-20AC column oven.

3. Results

3.1. Derivatization and LC–ESI-MS^n methodology

Derivatization of plasma sterols with 10 mM GP reagent in methanol containing 1% acetic acid was performed for 120 min [8], after which time the reaction mixture was injected for automated C$_{18}$-solid phase extraction (SPE) to remove excess derivatization reagent, with subsequent back-flushing of GP-tagged sterols onto a reversed phase C$_{18}$-HPLC column for chromatographic separation. Although the removal of plasma cholesterol prior to derivatization with an additional SPE step minimizes generation of cholesterol auto-oxidation products [29], we chose to perform our analysis without this step to ensure detection of sterols that otherwise may have been removed alongside the cholesterol. Detection of GP-tagged C4-7α-ol-3-one in plasma from a representative untreated CTX patient and cyp27A1 −/− mouse is shown with reconstructed ion chromatograms (RICs ± 5 ppm) derived from data generated in the Orbitrap mass analyzer (Fig. 2, upper RIC for CTX plasma, Panel C, and upper RIC for female cyp27A1 −/− mouse plasma, Panel D). In addition to expected presence of C4-7α-ol-3-one, we detected C4-3-one at elevated concentrations, particularly in the CTX plasma (Fig. 2, upper RIC for CTX plasma, Panel G, and upper RIC for cyp27A1 −/− mouse plasma, Panel H). Fragmentation routes for GP-tagged sterols are illustrated by the MS^2 and MS^3 spectra obtained for C4-3-one (Fig. 3; a major [M−79]$^+$ fragment ion is observed in MS^2 ([M]$^+$→) spectra, structurally informative fragment ions are observed in MS^3 ([M]$^+$ → [M−79]$^+$→) spectra). GP-tagged sterols were identified by comparison to authentic standard where available (for example with 5α-cholestan-3-one, Fig. 4) and by exact mass and MS^n data where no standard was available (for example with 7α,12α-dihydroxy-4-cholesten-3-one, Fig. 5).

3.2. Quantification

For the profiling experiments performed with the LTQ-Orbitrap Discovery a semi-quantitative determination of concentration was made for most compounds listed in Table 1, by isotope dilution mass spectrometry against known amounts of [^{2}H]7-labeled C4-7α-ol-3-one and C4-3-one internal standards. Peak areas obtained from RICs (±5 ppm) generated in the Orbitrap were used to calculate the concentration for GP-tagged 3-oxo-4-ene sterols according to equation: analyte peak area/IS peak area = analyte concentration/IS concentration. This equation is valid as GP-tagged 3-oxo-4-ene sterols have been shown to have an identical response factor [30]. For GP-tagged 3-oxo-5(H) saturated sterols the calculated concentrations were normalized to the response factor for 5α-cholestan-3-one according to the equation: (analyte peak area/IS peak area)/(5α-cholestan-3-one peak area/IS peak area) = analyte concentration/IS concentration. Concentrations were determined for C4-7α-ol-3-one, C4-3-one and 5α-cholestan-3-one by generating calibration curves. Acceptable

linearity (up to 10,000 ng/ml for C4-7α-ol-3-one and 2,000 ng/ml for C4-3-one and 5α-cholestan-3-one) was demonstrated for each calibration curve with characteristic correlation coefficients (r^2) >0.95. The within-run precision (RSD) for calculated GP derivative concentration from replicate analyses of a CTX sample is shown in Table 1.

We previously fully validated an LC–ESI-MS^2 method for quantification of GP-tagged C4-7α-ol-3-one in CTX plasma with a 4000 QTRAP operating in triple quadrupole mode [8]. We modified this method to include quantification of GP-tagged C4-3-one and 5α-cholestan-3-one in CTX patient and cyp27A1 −/− mouse plasma. Calibration curves were generated by performing a least-squares linear regression for calibrant peak area ratios obtained (sterol peak area/C4-3-one-d$_7$ peak area) versus concentration in ng/ml plasma. Acceptable linearity was demonstrated for each calibration curve (up to 2000 ng/ml) with characteristic correlation coefficients (r^2) >0.95. Plasma calibrators were included with each sample set and monitored over a month (RSD for all calibrators apart from LLOQ was <15% and accuracy was between 85–115%; data not shown). The LLOQ (with RSD <20%) for C4-3-one was 50 ng/ml and for 5α-cholestan-3-one was 100 ng/ml. To determine the effect of plasma matrix on detection of GP-tagged sterols, authentic standards were derivatized in the presence of commercially available plasma, and the ion abundance detected was compared to the ion abundance detected for authentic standard derivatized without plasma. Signal recovery was >80%, similar to results we previously observed for C4-7α-ol-3-one [8].

3.3. Applications of the methodology

We hypothesized derivatization with GP reagent would provide a window with which to examine the 3-oxo sterols that accumulate in CTX (Fig. 1) as Girard's reagent reacts with the sterol oxo moiety to enable selective ESI-MS^n analysis of these sterols. We profiled the 3-oxo-4-ene and 3-oxo-5(H) saturated sterols present in plasma from a representative untreated CTX patient and cyp27A1 −/− mice using GP derivatization and LC–ESI-MS^n analysis and were able to obtain semi-quantitative concentration estimates from data generated in the Orbitrap (data for cyp27A1 −/− mice shown in Table 1). The most noticeable gender difference was a higher concentration of bile acid precursors C4-7α-ol-3-one and 7α-hydroxy-5β-cholestan-3-one in plasma from female cyp27A1 −/− mice. We found concentrations of C4-7α-ol-3-one and 7α-hydroxy-5β-cholestan-3-one to be fairly comparable in cyp27A1 −/− mice and in the CTX patient (see also Fig. 2).

Concentrations of 12α-hydroxylated bile acid precursors were markedly lower in cyp27A1 −/− mouse plasma compared to those in the CTX patient, although they were elevated compared to cyp27A1 wild type littermates (data not shown). Concentrations of plasma 4,6-cholestadiene-3-one, C4-3-one and 5α-cholestan-3-one in the cyp27A1 −/− mice were around 14% of those in the CTX patient.

We further quantified plasma C4-7α-ol-3-one, C4-3-one and 5α-cholestan-3-one for a number of untreated CTX patients and female and male cyp27A1 −/− and cyp27A1 wild type mice via LC–ESI-MS^2 analysis performed with a 4000 QTRAP instrument and, in addition, quantified 5α-cholestanol and cholesterol in the plasma samples using GC-methodology (Table 2). The mean plasma C4-7α-ol-3-one, C4-3-one and 5α-cholestan-3-one concentrations obtained were similar to those determined from Orbitrap data, with the mean concentration of C4-7α-ol-3-one in the cyp27A1 −/− mice being 52% of the concentration in CTX patients, but 14.9-fold increased compared to wild type mice ($P = 0.016$). The concentrations of C4-3-one and 5α-cholestan-3-one in the cyp27A1 −/− mice were <25% of the concentrations in CTX patients, with C4-3-one
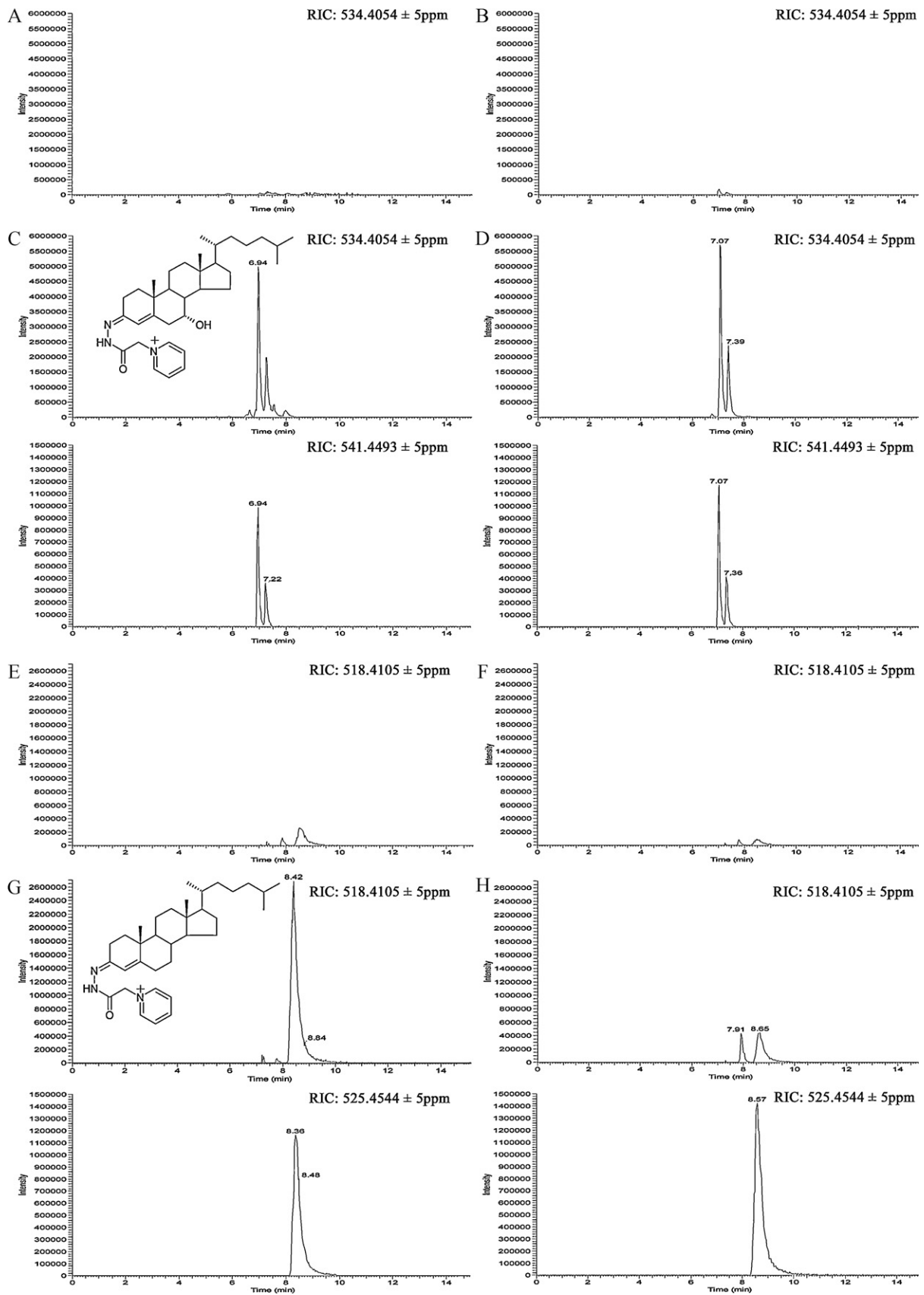
A.E. DeBarber et al. / J. Chromatogr. B 879 (2011) 1384–1392

Fig. 2. 7α-Hydroxy-4-cholesten-3-one and 4-cholesten-3-one present in plasma from untreated CTX patient and cyp27A1 −/− mice. Panels A & B and E & F are RICs from data generated in the Orbitrap analyzer for plasma from representative unaffected human and 24-month-old female wild type mouse, respectively. Panels C & D and G & H (upper chromatograms) are RICs for plasma from representative CTX affected patient and 24-month-old female cyp27A1 −/− mouse, respectively. GP-tagged C4-7α-ol-3-one (exact mass 534.4054) appears in chromatograms as *syn* and *anti* conformers eluting at 7 and 7.3 min. GP-tagged C4-3-one (exact mass 518.4105) appears in chromatograms as broad peak eluting at 8.4 min. Panels C & D and G & H (lower chromatograms) are RICs for [2H]7-labeled C4-7α-ol-3-one (exact mass 541.4493) and [2H]7-labeled C4-3-one (exact mass 525.4544) internal standards, respectively, spiked into plasma samples.
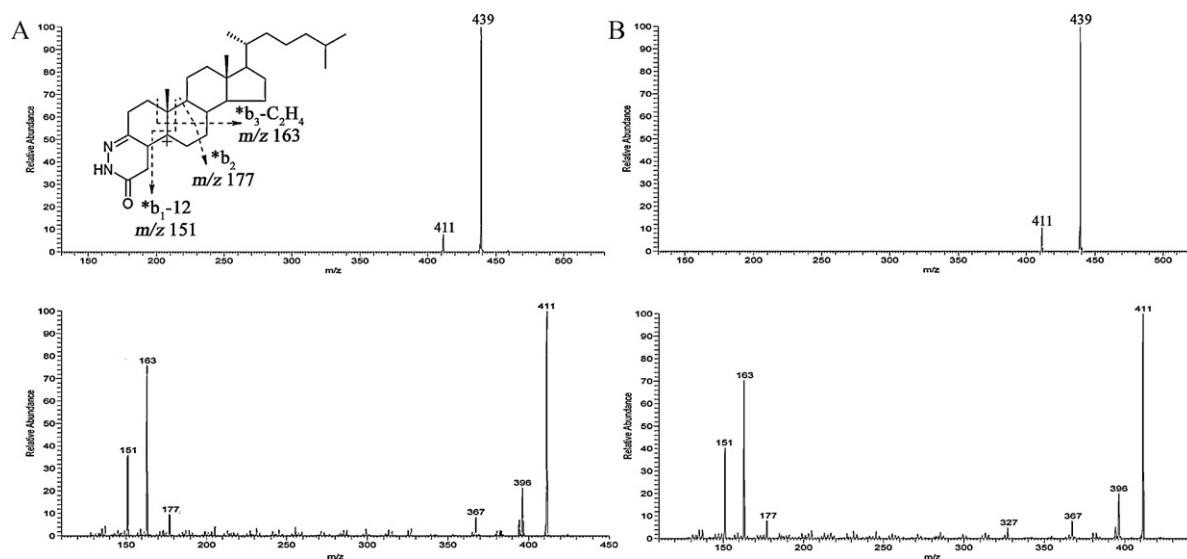
Fig. 3. Fragmentation routes for GP-tagged 3-oxo-4-ene sterols illustrated by 4-cholesten-3-one. Panel A is MS^2 (518→; upper panel) and MS^3 (518 → 439→; lower panel) spectra for GP-tagged C4-3-one from CTX plasma eluting at 8.4 min. Panel B is MS^2 and MS^3 spectra for GP-tagged authentic standard at same retention time. Major [M−79]$^+$ and [M−107]$^+$ fragment ions formed by the neutral loss of pyridine, and pyridine plus CO, respectively, are observed in MS^2 ([M]$^+$→) spectra; structure for [M−79]$^+$ ion is shown as *inset* to Panel A [29]. Formation of structurally informative fragment ions observed in MS^3 ([M]$^+$ → [M−79]$^+$→) spectra are indicated according to Griffiths et al. [29]. MS^n spectra were generated in LIT analyzer.

increased 4.7-fold ($P = 0.003$) and 5α-cholestan-3-one increased 1.7-fold ($P = 0.016$) compared to wild type mice. The mean concentration of 5α-cholestanol in the cyp27a −/− mice was 17% the concentration in CTX patients, but 1.6-fold increased compared to wild type mice ($P = 0.010$).

4. Discussion

We present here an example of incorporating a derivatization step for analysis with ESI-MS^n, not only to improve analytical sensitivity, but also to tag a specific class of molecules present in a genetic
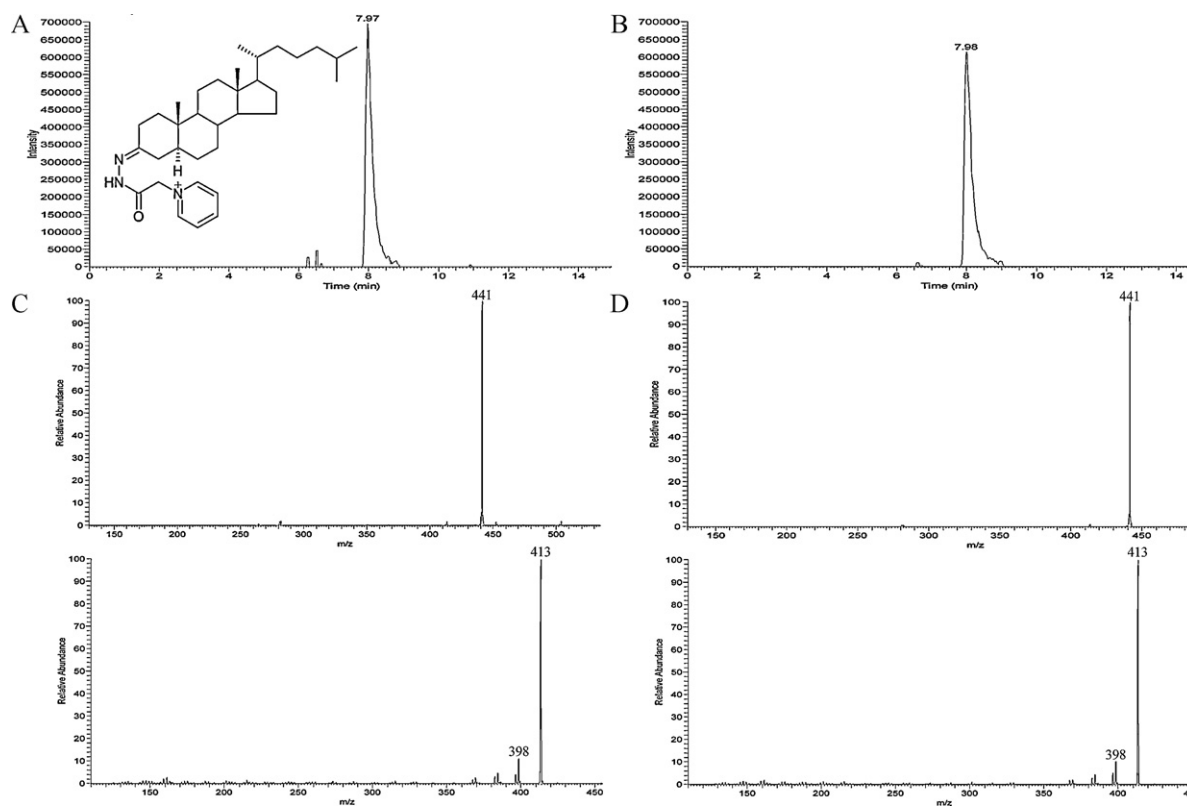

Fig. 4. 5α-Cholestan-3-one present in plasma from untreated CTX patient. Panels A and B are RICs from data generated in the Orbitrap analyzer for representative CTX plasma sample and authentic standard, respectively. GP-tagged 5α-cholestan-3-one appears in chromatogram as broad peak eluting at 8 min. Panel C is MS^2 (520→; upper panel) and MS^3 (520 → 441→; lower panel) spectra for GP-tagged 5α-cholestan-3-one from CTX plasma. Panel D is MS^2 and MS^3 spectra for GP-tagged authentic 5α-cholestan-3-one. Collision induced dissociation of [M−79]$^+$ ion observed in MS^2 spectra leads to formation of two ions in MS^3 spectra; m/z 413 corresponding to loss of pyridine plus CO [M−107]$^+$ and m/z 398, likely arising from loss of pyridine plus isocyanic acid [M−79−HNCO]$^+$.
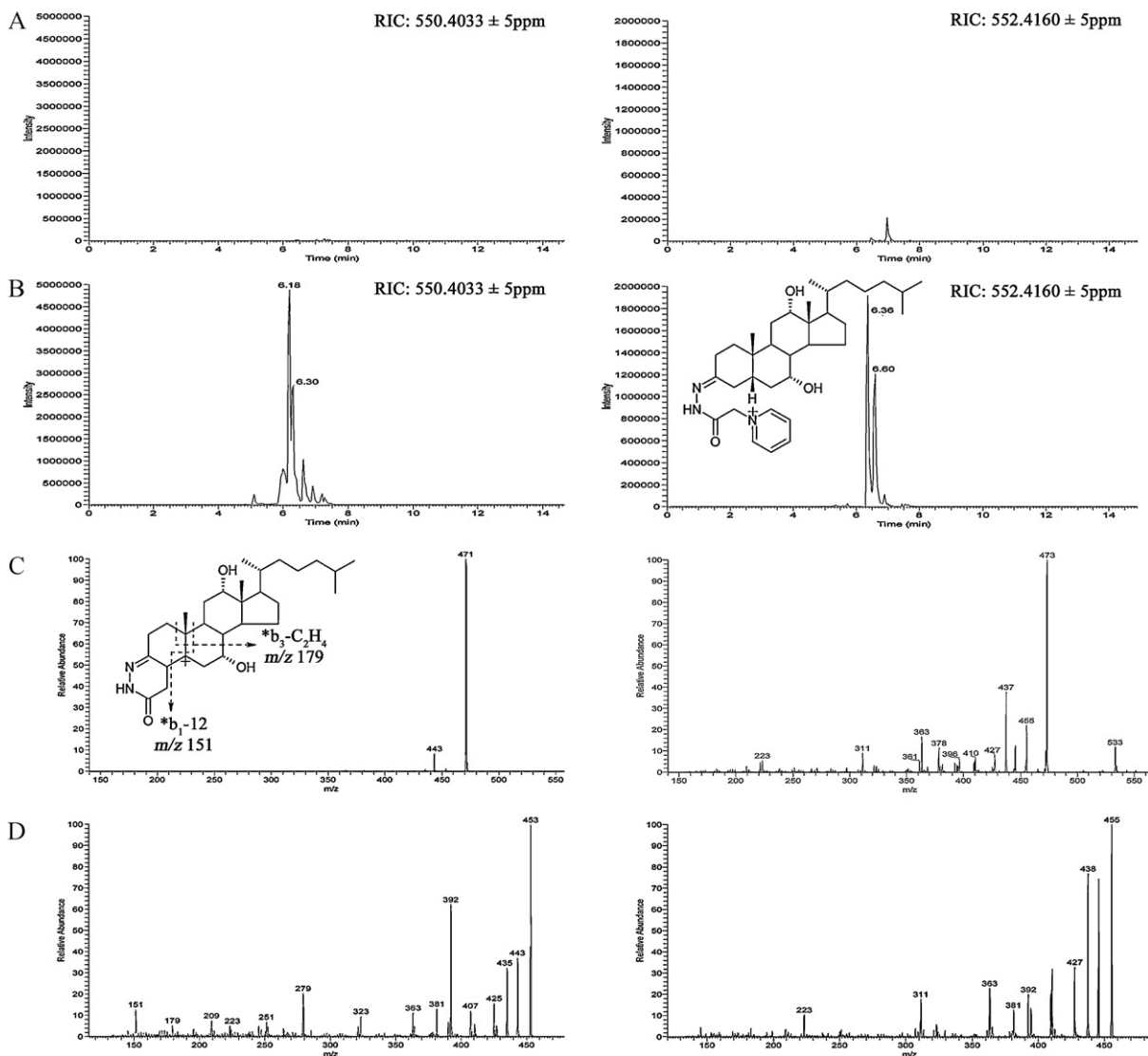
Fig. 5. 7α,12α-Dihydroxy-4-cholesten-3-one and 7α,12α-dihydroxy-5β-cholestan-3-one present in plasma from untreated CTX patient. Panels A and B are RICs from data generated in the Orbitrap analyzer for plasma from representative un-affected and CTX affected subject, respectively. Left panels; putative GP tagged 7α,12α-dihydroxy-4-cholesten-3-one appears in chromatogram as *syn* and *anti* conformer split peak eluting at 6.2–6.3 min. Right panels; GP-tagged 7α,12α-dihydroxy-5β-cholestan-3-one appears in chromatogram as peak eluting at 6.6 min (peak at 6.4 min is unidentified putative dihydroxy-5β-cholestan-3-one). Panel C is respective MS^2 spectra (550 → left panel, 552 → right panel) and Panel D is respective MS^3 spectra (550 → 471 → left panel; 552 → 473 → left panel). Formation of structurally informative fragment ions observed in MS^3 spectra for 7α,12α-dihydroxy-4-cholesten-3-one $[M−79]^+$ ion are indicated (*inset* to Panel C); including $^*b_3 − C_2H_4$ fragment observed at m/z 179 indicating presence of 7α-hydroxyl group [29]. There is no $^*c_2 + 2H−H_2O$ fragment observed at m/z 231 (from cleavage of C-ring) [29], indicating C-ring is modified, likely with 12α-hydroxyl group. The presence of two hydroxyl groups is consistent with observation of characteristic $[M−79−(nH_2O)]^+$ and $[M−107−(nH_2O)]^+$ ions [29]. GP-tagged 7α,12α-dihydroxy-5β-cholestan-3-one from CTX plasma was identified by comparison to GP-tagged authentic standard. Fragment ions observed in the MS^3 spectrum include m/z $[M−79−(nH_2O)]^+$ and $[M−107−(nH_2O)]^+$ ions indicative of two hydroxyl groups. Low abundance ions at m/z 392 and 394 most likely arise from neutral loss of pyridine, NH_3, CO and two molecules of water $[M−79−NH_3−CO−2H_2O]^+$ and loss of pyridine, isocyanic acid and water $[M−79−HNCO−2H_2O]^+$, respectively.

disorder. The selective generation of GP-tagged 3-oxo-4-ene and 3-oxo-5(H) saturated plasma sterols enabled ESI-MS^n detection of proposed *in vivo* sterol intermediates in CTX biochemical pathways (shown in grey, Fig. 1). Sterol detection was accomplished with good sensitivity using conventional HPLC-ESI methodology, despite the presence of a large excess of cholesterol. The signal enhancement factor for Girard derivatization of C4-7α-ol-3-one and analysis with ESI-MS/MS relative to analysis of underivatized C4-7α-ol-3-one with APCI-MS/MS was >30-fold. Some sterols were identified by comparison with authentic standards and others by information provided from LC–ESI-MS^n experiments performed with the LTQ-Orbitrap Discovery instrument.

To our knowledge measurement of elevated C4-3-one or 5α-cholest-3-one has not been previously described in blood or tissues from CTX patients, although these sterols are known to be immedi-ate precursors of 5α-cholestanol based on [^{14}C]4-labeled C4-3-one dosing experiments [10,11] and *in vitro* studies [14]. It is of interest to note that despite comparable plasma cholesterol concentrations between CTX patients and an unaffected subject, there is a large difference in C4-3-one concentrations (Table 1). Elevated C4-7α-ol-3-one and 4,6-cholestadiene-3-one were previously detected in CTX serum [2] and an alternative pathway to C4-3-one was proposed from C4-7α-ol-3-one through 4,6-cholestadiene-3-one [9].

In accordance with previous studies in cyp27A1 −/− mice [20], we determined the mean plasma concentration of C4-7α-ol-3-one in 24 month old cyp27A1 −/− mice was 52% of the plasma concentration in CTX patients, compared with a plasma concentration of 5α-cholestanol in cyp27A1 −/− mice that was only 17% of the concentration in CTX patients. Female 12 month old cyp27A1 −/− mice were reported to display marked cere-

Table 1
Sterols identified in plasma from untreated CTX patient and 24 month old cyp27A1 −/− mice utilizing data generated with LTQ-Orbitrap instrument.

GP derivative	Formula	Exact mass	RT (min)	Conc. for representative CTX patient (ng/ml)	Method RSD[a] (%)	Mean conc. ($n=3$) male cyp27A −/− mice (ng/ml)	Mean conc. ($n=3$) female cyp27A −/− mice (ng/ml)
4,6-Cholestadiene-3-one 3GP[b,e,f,i]	$C_{34}H_{50}N_3O_1^+$	516.3948	7.6	1215	8.5	150	187
4-Cholesten-3-one 3GP[b,e]	$C_{34}H_{52}N_3O_1^+$	518.4105	8.0	4662	2.2	725	539
5α-Cholestan-3-one 3GP[b,e,h,i]	$C_{34}H_{54}N_3O_1^+$	520.4261	8.2	407	2.7	77	35
7α-Hydroxy-4-cholesten-3-one 3GP[c,e,g]	$C_{34}H_{52}N_3O_2^+$	534.4054	7.2	8842	8.9	2431	4344
7α-Hydroxy-5β-cholestan-3-one 3GP[c,d,h,i]	$C_{34}H_{54}N_3O_2^+$	536.4211	7.3	3231	9.0	2740	5031
7α,12α-Dihydroxy-4-cholesten-3-one 3GP[c,d,g,h,i]	$C_{34}H_{52}N_3O_3^+$	550.4033	6.2	2098	8.8	198	291
Putative dihydroxy 5β-cholestan-3-one 3GP[c,d,h,i,j]	$C_{34}H_{54}N_3O_3^+$	552.4160	6.2	848	3.9	106	99
7α,12α-Dihydroxy 5β-cholestan-3-one 3GP[c,e,h,i]	$C_{34}H_{54}N_3O_3^+$	552.4160	6.4	1282	6.7	ND	ND

ND, not detected.

[a] RSD is for representative CTX sample calculated concentration (within-run relative standard deviation for three replicates).

[b] Quantitative estimate was based on area ratio of analyte to 4-cholesten-3-one-d$_7$ internal standard (formula $C_{34}D_7H_{45}N_3O_1^+$, exact mass 525.4544).

[c] Quantitative estimate was based on area ratio of analyte to 7α-hydroxy-4-cholesten-3-one-d$_7$ internal standard (formula $C_{34}D_7H_{45}N_3O_2^+$, exact mass 541.4493).

[d] Identification based on exact mass and MS^n spectra.

[e] Identification based on comparison with authentic standard.

[f] 4,6-Cholestadien-3-one levels augmented by significant dehydration of C4-7α-ol-3-one under our derivatization conditions (<20% of 4,6-cholestdien-3-one response by comparison with dehydration of C4-7α-ol-3-one authentic standard, data not shown). Dehydration of C4-7α-ol-3-one is negligible in plasma stored at −20 °C for up to 10 months [26].

[g] Resolved *syn* and *anti* conformers.

[h] Not detected in plasma from unaffected subjects.

[i] Not detected in plasma from cyp27A1 +/+ mice.

[j] $[M-79-(n18)]^+$ and $[M-107-(n18)]^+$ fragment ions observed in MS^3 ($[M]^+ \rightarrow [M-79]^+ \rightarrow$) spectra consistent with two hydroxyl groups.

bral accumulation of 5α-cholestanol [20], although this was small in comparison to the accumulation in CTX patients. The difference in cerebral accumulation was hypothesized to be due to decreased 7α-hydroxylation in the mice, with decreased transfer of C4-7α-ol-3-one (and 7α-hydroxycholesterol) across the blood brain barrier. As the concentration of C4-7α-ol-3-one in cyp27A1 −/− mice is around half the concentration found in CTX patients, but the concentrations of 4,6-cholestadiene-3-one, C4-3-one and 5α-cholest-3-one range from a quarter to a fifth, we propose differences between the cyp27A1 −/− mouse and human disease may reside in decreased enzyme-catalyzed conversion of C4-7α-ol-3-one to 4,6-cholestdiene-3-one and C4-3-one or more efficient removal of these sterols from the alternative pathway to 5α-cholestanol in cyp27A1 −/− mice.

GP derivatization and LC–ESI-MS^n analysis also enabled the detection in plasma of intermediates in the neutral bile acid pathway (Fig. 1). The cyp27A1 −/− mice displayed quantitative differences in bile acid precursor profiles when compared with CTX patients, notably decreased 12α-hydroxylated intermediates like 7α,12α-dihydroxy-4-cholesten-3-one and 7α,12α-dihydroxy-5β-cholestan-3-one. Although 7α,12α-dihydroxy-4-

cholesten-3-one, 5β-cholestan-3α,7α,12α-triol and 5β-cholestan-3α,7α-diol were previously detected at high concentrations in plasma and liver tissue from CTX patients [4–6], to our knowledge elevated plasma 7α,12α-dihydroxy-5β-cholestan-3-one and 7α-hydroxy-5β-cholestan-3-one have not been previously reported.

A fragmentation route for GP-tagged 3-oxo-4-ene sterols has been proposed with the structure for $[M-79]^+$ ion shown as an *inset* to Panel A (Fig. 3) [29]. GP-tagged 3-oxo-5(H) saturated sterols fragment in an alternate manner with fragment ions observed in the MS^2 and MS^3 spectra that are similar in nature. The MS^2 ($[M]^+ \rightarrow$) spectra are dominated by $[M-79]^+$ fragment ions (formation of a $[M-79]^+$ fragment ion for GP-tagged 5α-cholestan-3-one was previously noted [29]) and the MS^3 ($[M]^+ \rightarrow [M-79]^+ \rightarrow$) spectra contain $[M-107]^+$ ions. There is an absence of characteristic 3-oxo-4-ene b ions indicating fragmentation likely does not involve B ring cleavage. There is also little evidence of C and D ring cleavage, except in the case of GP-tagged 7α,12α-dihydroxy-5β-cholestan-3-one. Modification of B and C rings by introduction of hydroxyl groups at C7 and C12 (Fig. 5) leads to formation of characteristic $[M-79-(n18)]^+$ and $[M-107-(n18)]^+$ fragment ions [29]. Overall

Table 2
Concentration of 5α-cholestanol precursors in plasma from untreated CTX patients and 24-month old cyp27A1 −/− mice.

	7α-Hydroxy-4-cholesten-3-one[a,b] (ng/ml)	4-Cholesten-3-one[a,c,d] (ng/ml)	5α-Cholestan-3-one[a,c,d] (ng/ml)	5α-Cholestanol[e] (μg/dl)	Cholesterol[e] (mg/dl)
Untreated CTX patients ($n=4$)	5675 ± 1975 (3720–7860)	1207 ± 302 (918–1580)	342 ± 90 (267–461)	3040 ± 910 (2510–4400)	148 ± 11 (132–156)
Representative unaffected subject	148	94	ND	220[f]	151
Female cyp27A1 −/− mice ($n=3$)	3897 ± 1952 (2740–6150)	170 ± 49 (113–201)	71 ± 10 (48–83)	329 ± 108 (224–440)	36 ± 11 (26–48)
Female cyp27A1 +/+ mice ($n=3$)	258 ± 124 (138–385)	42 ± 16 (25–55)	37 ± 10 (27–46)	228 ± 96 (171–339)	86 ± 42 (56–134)
Male cyp27A1 −/− mice ($n=3$)	2018 ± 1555 (694–3730)	115 ± 42 (83–162)	97 ± 14 (85–112)	706 ± 198 (518–913)	70 ± 8 (65–79)
Male cyp27A1 +/+ mice ($n=3$)	140 ± 115 (65–272)	17 ± 20 (6–41)	63 ± 15 (48–78)	405 ± 58 (344–460)	64 ± 15 (50–79)

Mean ± S.D. and (range of results) are given; ND, not detected.

[a] Analysis performed with 4000 QTRAP instrument scanning in triple-quad mode.

[b] Free sterol; quantification based on area ratio of 7α-hydroxy-4-cholesten-3-one to 7α-hydroxy-4-cholesten-3-one-d$_7$ internal standard synthesized as described previously [8].

[c] Free sterols; quantification was based on area ratio of sterol to 4-cholesten-3-one-d$_7$ internal standard.

[d] LLOQ for C4-3-one 50 ng/ml, for 5α-cholestan-3-one 100 ng/ml.

[e] Hydrolyzed sterols; quantification was by GC–FID and GS–MS.

[f] Normally <600 μg/dl and for CTX between 1300 and 15,000 μg/dl [9].

less structurally informative fragments are present the MS^3 spectra than for the corresponding 3-oxo-4-enes.

A limitation of the experiments we describe was the focus on 3-oxo-4-ene and 3-oxo-5(H) saturated sterols and bile alcohols, however these experiments could be easily modified to also examine 3α-hydroxy-5β(H) bile alcohols present in CTX, for example 3α,7α,12α-trihydroxy-5β-cholestane and 3α,7α-dihydroxy-5β-cholestane (by conversion to 3-oxo-5β(H) bile alcohols using 3α-hydroxysteroid dehydrogenase as described for synthesis of 7α,12α-dihydroxy-5β-cholestan-3-one in methods section [25]). Such experiments are underway in our laboratory and also possess the advantage that cholesterol in the samples remains underivatized.

In conclusion, we report here that GP derivatization of plasma and high resolution exact mass LC–ESI-MS^n analysis can be utilized to selectively profile the free 3-oxo sterol signature present in the systemic circulation of untreated CTX patients and in cyp27A1 −/− mice, even without removal of cholesterol, which is present in great excess. The techniques we describe facilitate the study of sterol and bile acid pathways in CTX, and should lead to improvements in screening, diagnosis, and treatment of this debilitating disease.

Acknowledgements

Appendix A. Supplementary data

Supplementary data associated with this article can be found, in the online version, at doi:10.1016/j.jchromb.2010.11.019.

References

[1] J.H. Menkes, J.R. Schimschock, P.D. Swanson, Arch. Neurol. 19 (1968) 47.
[2] I. Bjorkhem, S. Skrede, M.S. Buchmann, C. East, S. Grundy, Hepatology 7 (1987) 266.
[3] S. Skrede, M.S. Buchmann, I. Bjorkhem, J. Lipid Res. 29 (1988) 157.
[4] I. Bjorkhem, H. Oftebro, S. Skrede, J.I. Pedersen, J. Lipid Res. 22 (1981) 191.
[5] A. Honda, G. Salen, Y. Matsuzaki, A.K. Batta, G. Xu, E. Leitersdorf, G.S. Tint, S.K. Erickson, N. Tanaka, S. Shefer, J. Lipid Res. 42 (2001) 291.
[6] P.T. Clayton, A. Verrips, E. Sistermans, A. Mann, G. Mieli-Vergani, R. Wevers, J. Inherit. Metab. Dis. 25 (2002) 501.
[7] S. Skrede, I. Bjorkhem, M.S. Buchmann, G. Hopen, O. Fausa, J. Clin. Invest. 75 (1985) 448.
[8] A.E. DeBarber, W.E. Connor, A.S. Pappu, L.S. Merkens, R.D. Steiner, Clin. Chim. Acta 411 (2010) 43.
[9] I. Bjorkhem, K. Muri Boberg, E. Leitersdorf, The Online Metabolic & Molecular Bases of Inherited Disease, 2001, p. 2961 (Chapter 123).
[10] G. Salen, S. Shefer, G.S. Tint, Gastroenterology 87 (1984) 276.
[11] S. Skrede, I. Bjorkhem, J. Biol. Chem. 257 (1982) 8363.
[12] G.M. Tomkins, C.W. Nichols Jr., D.D. Chapman, S. Hotta, I.L. Chaikoff, Science 125 (1957) 936.
[13] C.W. Nichols Jr., S. Lindsay, D.D. Chapman, I.L. Chaikoff, Circ. Res. 8 (1960) 16.
[14] S. Shefer, S. Hauser, E.H. Mosbach, J. Biol. Chem. 241 (1966) 946.
[15] S. Shefer, S. Hauser, E.H. Mosbach, J. Lipid Res. 7 (1966) 763.
[16] M.S. Buchmann, I. Bjorkhem, S. Skrede, Biochim. Biophys. Acta 922 (1987) 111.
[17] I. Bjorkhem, M. Buchmann, S. Bystrom, J. Biol. Chem. 267 (1992) 19872.
[18] W.J. Griffiths, M. Hornshaw, G. Woffendin, S.F. Baker, A. Lockhart, S. Heidelberger, M. Gustafsson, J. Sjovall, Y. Wang, J. Proteome Res. 7 (2008) 3602.
[19] C.H. Shackleton, H. Chuang, J. Kim, X. de la Torre, J. Segura, Steroids 62 (1997) 523.
[20] A. Bavner, M. Shafaati, M. Hansson, M. Olin, S. Spitzen, V. Meiner, E. Leitersdorf, I. Bjorkhem, J. Lipid Res 51 (2010) 2722.
[21] A. Honda, K. Yamashita, T. Hara, T. Ikegami, T. Miyazaki, M. Shirai, G. Xu, M. Numazawa, Y. Matsuzaki, J. Lipid Res. 50 (2009) 350.
[22] S. Dubrac, S.R. Lear, M. Ananthanarayanan, N. Balasubramaniyan, J. Bollineni, S. Shefer, H. Hyogo, D.E. Cohen, P.J. Blanche, R.M. Krauss, A.K. Batta, G. Salen, F.J. Suchy, N. Maeda, S.K. Erickson, J. Lipid Res. 46 (2005) 76.
[23] S.K. Erickson, S.R. Lear, S. Deane, S. Dubrac, S.L. Huling, L. Nguyen, J.S. Bollineni, S. Shefer, H. Hyogo, D.E. Cohen, B. Shneider, E. Sehayek, M. Ananthanarayanan, N. Balasubramaniyan, F.J. Suchy, A.K. Batta, G. Salen, J. Lipid Res. 44 (2003) 1001.
[24] A.K. Bhattacharyya, D.S. Lin, W.E. Connor, J. Lipid Res. 48 (2007) 185.
[25] M. Une, J. Harada, T. Mikami, T. Hoshita, J. Chromatogr. B: Biomed. Appl. 682 (1996) 157.
[26] C. Galman, I. Arvidsson, B. Angelin, M. Rudling, J. Lipid Res. 44 (2003) 859.
[27] A. Lovgren-Sandblom, M. Heverin, H. Larsson, E. Lundstrom, J. Wahren, U. Diczfalusy, I. Bjorkhem, J. Chromatogr. B: Anal. Technol. Biomed. Life Sci. 856 (2007) 15.
[28] M. Ogundare, S. Theofilopoulos, A. Lockhart, L.J. Hall, E. Arenas, J. Sjovall, A.G. Brenton, Y. Wang, W.J. Griffiths, J. Biol. Chem. 285 (2010) 4666.
[29] W.J. Griffiths, Y. Wang, G. Alvelius, S. Liu, K. Bodin, J. Sjovall, J. Am. Soc. Mass Spectrom. 17 (2006) 341.
[30] K. Karu, M. Hornshaw, G. Woffendin, K. Bodin, M. Hamberg, G. Alvelius, J. Sjovall, J. Turton, Y. Wang, W.J. Griffiths, J. Lipid Res. 48 (2007) 976.